

## AN OPTIMIZATION APPROACH TO MODELING SEA ICE DYNAMICS. PART 1: LAGRANGIAN FRAMEWORK\*

HELGA S. HUNTLEY<sup>†</sup>, ESTEBAN G. TABAK<sup>‡</sup>, AND EDWARD H. SUH<sup>‡</sup>

**Abstract.** A new model for the dynamics of sea ice is proposed. The pressure field, instead of being derived from a local rheology as in most existing models, is computed from a global optimization problem. Here the pressure is seen as emerging not from an equation of state but as a Lagrange multiplier that enforces the ice's resistance to compression while allowing divergence. The resulting variational problem is solved by minimizing the pressure globally throughout the domain, constrained by the equations of momentum and mass conservation, as well as the limits on ice concentration (which has to stay between 0 and 1). This formulation has an attractive mathematical elegance while being physically motivated. Moreover, it leads to an analytic formulation that is also easily implemented in a numerical code, which exhibits marked stability and is suited to capturing discontinuities. In order to test the theory, the equations for a one-dimensional model are cast in terms of Lagrangian mass coordinates. The solution to the minimization problem is compared to an exact analytic solution derived using jump conditions in a simple test case. Another case is examined, which is somewhat more complicated but still allows our physical intuition to verify the qualitative results of the model. Good agreement is found. A final validation is performed by a comparison with a particle-based model, which tracks individual ice floes and their inelastic interaction in a one-dimensional domain.

**Key words.** ice dynamics, rheology, Lagrangian fluid dynamics

**AMS subject classifications.** 76M30, 86A05

**DOI.** 10.1137/040621156

**1. Introduction.** Unlike the dynamics of the ocean waters, sea ice dynamics is relatively little understood. Part of the problem is that ice is a somewhat peculiar substance; it is neither hard as steel, nor elastic like rubber, nor completely fluid like a liquid. Colliding ice floes do not behave like the familiar billiard balls with perfectly round shapes and elastic collisions. An additional challenge for the modeler interested in the large scales of the whole Arctic, or at least an entire strait, is the limit of resolution. It is impossible to follow individual ice floes. Instead the behavior of a field of floes on the order of several square kilometers must be summarized by tracking an average velocity (mass-weighted), a thickness distribution, and the concentration of ice in the grid box. On this scale, one can no longer rely on first physical principles for the solid bodies making up the ice. So what are the laws of physics describing the motion of a half empty box of solid substance that strongly resists compression up to its breaking point but is easily pulled apart due to a multitude of fractures?

Scientists over the years have suggested various analogies, two of which have shown enough promise to have stood the test of time: ice as a fluid, and ice as a granular material. Most models today following the first of these approaches in some way relate back to the sea ice rheology proposed by Hibler in [3], based on the postulate

\*Received by the editors December 20, 2004; accepted for publication (in revised form) August 30, 2006; published electronically February 15, 2007. This article derives from work done as part of the Ph.D. thesis of Helga Schaffrin Huntley, while partially supported by the NSF VIGRE program.

<http://www.siam.org/journals/siap/67-2/62115.html>

<sup>†</sup>Department of Applied Mathematics, University of Washington, Box 352420, Seattle, WA 98195-2420 ([helga@amath.washington.edu](mailto:helga@amath.washington.edu)).

<sup>‡</sup>Department of Mathematics, Courant Institute of Mathematical Sciences, New York University, 251 Mercer St., New York, NY 10012 ([tabak@cims.nyu.edu](mailto:tabak@cims.nyu.edu), [ehs@nyu.edu](mailto:ehs@nyu.edu)). The work of the second author was partially supported by grants from the NSF Division of Applied Mathematics.

that ice behaves like a nonlinear viscous-plastic compressible fluid. Improvements have been made on the original model, including an extension with an elastic component to the constitutive law, but the essential character has been maintained (cf., for example, [5]). Parts of the “state-of-the-art” formulation of the rheology are based on the observations that ice resists compression up to a breaking point (plastic); the viscous character is added to avoid multivalued functions, while the elastic terms are mostly introduced for greater numerical stability. While the numerical results are generally good, to some extent this is due to parameter tuning to available (though often scarce) data.

Models based on a cavitating fluid rheology also fall into this first category. They do not naturally incorporate shear strength (although this has been partially addressed), but are computationally somewhat simpler and less expensive, making use of an iterative correction scheme. These models also have had some success in reproducing realistic ice transport (cf., for example, [2]).

In the second category, a granular rheology has been developed by Tremblay and Mysak [11], as well as others (e.g., the CRREL<sup>1</sup> uses a high-resolution granular sea ice model, based on [4]). These are better equipped to handle such tasks as tracking leads in an ice field, although a much higher resolution is required for such problems.

Model intercomparison studies have found that the choice of rheology has a significant impact on the model output; see, e.g., [6] and [1]. A somewhat more comprehensive study, SIMIP, the Sea Ice Model Intercomparison Project, was carried out in the late 1990s. It compared viscous-plastic, cavitating fluid, compressible Newtonian fluid, and free-drift with velocity corrections rheologies. Overall, it was found that the viscous-plastic rheology produced the best results, while the free-drift simulation showed large errors in ice drift, thicknesses, and export through the Fram Strait, the compressible Newtonian model yielded excessive ice thickness build-up in the central Arctic, and the cavitating fluid rheology resulted in errors in ice drift and the thickness pattern. However, in some respects none of the models gave entirely satisfactory results. Thus, for example, in an analysis of the summer sea ice extent anomalies, none of the model results lies consistently within the error band of the observations (from satellite data). The same is true for anomalies of annual mean ice thickness in the Beaufort Sea (where the observational data was collected with upward looking sonars). These results were reported in [7]. The present work on a new approach to treating the internal stress term for sea ice dynamics was motivated in part by the realization that existing models not only disagree significantly with each other but also have remaining difficulties reproducing some observed phenomena, such as the formation of ice arches in the Canadian Arctic Archipelago.

We have chosen to follow the first approach, an analogy to fluids, but are employing a novel global formulation of the rheology as the solution to an optimization problem. We attempt to build a theoretical framework, with supporting numerical experiments, to reproduce and explain the relevant observations of sea ice dynamics. We start with the analogy that ice behaves like a fluid with some special properties. In particular, sea ice exhibits semi-incompressibility: It allows divergence without much resistance, due to the many cracks and leads within the ice pack, but strongly resists convergence at high concentration. The goal is to find an expression for the pressure enforcing this semi-incompressibility, which is mathematically elegant and computationally efficient, allowing for clean analytic solutions in simple cases and numerical simulations of more complicated ones. Reliance on parameterization is to

---

<sup>1</sup>Cold Regions Research and Engineering Laboratory of the US Army Corps of Engineers.

be minimized. To this end, we start with the fluid equations and investigate how they need to be modified to retain validity in the context of sea ice. The central hypothesis is that the pressure acting within the ice field is the minimum necessary to prevent the unrealistic situation of multiple floes occupying the same space. In other words, the pressure term enforces the condition that the area fraction covered by ice (the concentration) may not exceed 1. Our formulation permits the calculation of the pressure using linear programming, benefiting from existing schemes, without tuning to observations.

The goal of the work reported in this article is to demonstrate the feasibility of having the pressure solve a variational problem. To this end, we concentrate on the simplest possible scenario, one of unforced one-dimensional flows, with uniform ice thickness and infinite yield pressure, so that no crushing occurs. A companion paper (Part 2) discusses the effects of ice yielding. Current work, which will be reported in later publications, involves extending the flow to two horizontal dimensions and allowing for nontrivial ice thickness distributions. A more detailed discussion of many of the results in this paper can be found in [9]. Here we will consider a simplified Lagrangian system, which allows both analytic solutions to basic test cases and a straightforward numerical implementation to be tested against a particle-based model resolving individual ice floes. As will be shown, the minimal pressure hypothesis leads to very encouraging results in the studied test cases, justifying further investigation of this particular rheology.

**2. Coarse grained ice dynamics as fluid dynamics.** We shall use the following variables:

$c$  = concentration of ice (fraction of sea surface area covered by ice),

$h$  = average thickness of the ice,

$\mathbf{u} = (u, v)$  = horizontal velocities,

$S$  = sources – sinks of ice (melting and freezing, precipitation),

$F^x, F^y$  = sum of zonal, meridional forces

(Coriolis, wind, currents, sea surface tilt, pressure).

Note that in the following we are taking the density of ice  $\rho$ , which is nearly constant, to be identically 1. This convention simplifies the notation and has no influence on the qualitative results we are interested in. Equivalently, one can describe this as absorbing the density into the thickness parameter, so that  $h$  is measured in kg/m<sup>2</sup>.

Most of today's sea ice dynamics models employ a thickness distribution function to allow for ice of various thicknesses in any one grid cell (cf. [10]). For the simple model we are building here to verify the minimal pressure hypothesis, we will not include this level of complexity at this time. Similarly, we are not concerned with tracking a velocity distribution within a grid cell, but assume the velocities  $u$  and  $v$  to be mass-averaged velocities for the entire box.

In Eulerian coordinates, the mass conservation and momentum conservation equations can be written as

$$(1) \quad (ch)_t + \nabla \cdot (chu) = S,$$

$$(2) \quad (chu)_t + \nabla \cdot (chu\mathbf{u}) = F^x,$$

$$(3) \quad (chv)_t + \nabla \cdot (chv\mathbf{u}) = F^y,$$

where the product  $ch$  (really  $ch\rho$ ) plays the role of a density in analogy with the conventional fluid equations.

What differentiates the case of ice from standard fluids is that, in addition to these two conservation laws, we also have the constraint that  $c$  can vary (unlike the density of incompressible fluids) but may not exceed 1, which is enforced by a pressure force. In this paper, we want to investigate the nature of this pressure force and a new way to calculate it. To isolate this issue, we will consider the one-dimensional case without sources or sinks ( $S = 0$ ). By defining  $F = F^x/(ch)$ , subtracting  $u$  times (1) from (2), and dividing by  $ch$ , the system reduces to

$$(4) \quad (ch)_t + (chu)_x = 0,$$

$$(5) \quad u_t + u u_x = F.$$

Notice that, even if  $F$  were given (which it is not, since the pressure is one of the variables to be determined), this system has only two equations but three unknowns. Mass conservation alone does not provide for a way to evolve the fractional area  $c$  and the mean thickness  $h$  separately. Extra physical assumptions are necessary to complete the system's description. In the absence of crushing (or sources or sinks), a natural assumption is that the thickness  $h$  is advected with ice floes:

$$(6) \quad h_t + u h_x = 0.$$

In words, when a pack of floes is pulled apart, the floes do not become thinner: It is the space between them that increases, thus reducing the fractional area coverage  $c$ . (The assumption of advection of  $h$  is relaxed in Part 2 of this work.)

**3. The Lagrangian formulation.** To gain further insight into this system and to make analytic solutions easier to obtain, we introduce the Lagrangian mass coordinates<sup>2</sup>

$$(7) \quad \begin{cases} \xi = \int_0^x ch d\hat{x}, \\ \tau = t. \end{cases}$$

The resulting Lagrangian equations in these coordinates for one-dimensional ice motion without sources or sinks are

$$(8) \quad \left( \frac{1}{ch} \right)_\tau = u_\xi,$$

$$(9) \quad u_\tau = F.$$

(See the appendix for the derivation.)

Introducing the variable  $k \equiv \frac{1}{ch} - 1$  yields

$$(10) \quad k_\tau = u_\xi,$$

$$(11) \quad u_\tau = F.$$

While these equations have a beguilingly simple form, we have now lost sight of the crucial variable  $c$ , which we have to constrain. We would like to translate this

---

<sup>2</sup>Lagrangian mass coordinates are often used in astronomical papers, as well as in studies of hydrodynamics; cf., for just one example, [12].

constraint into a constraint on  $k$ . In the case where  $h \equiv 1$ , this is easily done: The constraint  $c \leq 1$  now becomes  $k \geq 0$ . An extension to varying  $h$  is straightforward (the constraint becomes  $k \geq \frac{1-h}{h}$ ), but it obscures the pressure effect. Thus, for easier visualization, we shall focus on the particular case of constant ice thickness  $h \equiv 1$ . (Variations in ice thickness are reintroduced in Part 2.) Note that, in addition to excluding melting and freezing processes as well as precipitation, fixing  $h$  also eliminates crushing from the problem. While a realistic and versatile ice model will ultimately require us to bring these components back, the nature of the pressure force and its role in ice dynamics can more easily be investigated in isolation. For this purpose we make one more simplification and isolate the pressure term by setting all other forces equal to zero.

What form this pressure term should take is not immediately obvious. Various suggestions have been made over the years, which fall into two main categories. On the one hand, there are the viscous-plastic or viscous-plastic-elastic models, which all hark back to the original formulation in terms of the stress/strain yield curve in [3]. On the other hand are the cavitating fluid models, which calculate the pressure in a series of correction steps (cf. [2]). While these are backed up by more or less realistic model outputs, they are dependent on empirical parameter tuning and exhibit some numerical shortcomings in the first case and follow an iterative relaxation scheme in the latter. The goal of our approach is to minimize the reliance on empirical parameter tuning and iterative schemes to the extent possible. Our physical intuition tells us that the pressure does not act unless it is necessary to prevent ice concentration from exceeding 1, i.e., to prevent two ice floes from occupying the same space. In other words, while  $c$  is far from 1, the pressure force  $F = 0$ , and the flow follows  $u_\tau = 0$ . Each parcel's velocity does not change with time. By adding a pressure to the system, we would like to deviate as little as possible from this route while satisfying the constraint. This suggests a mathematical formulation as a constrained optimization problem, where the pressure is defined as a Lagrange multiplier.

We do not expect the pressure force to push the ice apart, as any elastic rheology would. Rather, it builds up as the ice converges, solely to prevent multiple floes from occupying the same space. The goal then is to find a pressure that allows us to minimize the change in  $u$  over time. Lagrange multipliers were invented for just such constrained optimization problems. Here we have two constraints acting on  $u$ , the equation for the evolution of  $k$  and the lower limit on  $k$ . Since  $k$  is defined at each point  $\xi$ , this in fact amounts to infinitely many constraints, one for each  $k(\xi)$ .

A note on notation: In the following (except for section 9), we will be discussing only the Lagrangian formulation of the problem. Thus, we will simplify our notation by replacing the Greek letters for the independent variables by their Roman cousins again, i.e., by writing the Lagrangian mass coordinate  $\xi$  as  $x$  and the Lagrangian time coordinate  $\tau$  as  $t$ .

#### 4. Pressure as a Lagrange multiplier.

The problem is at each time  $t$  to

$$(12) \quad \text{minimize} \quad \|u_t\|,$$

$$(13) \quad \text{given} \quad k_t = u_x,$$

$$(14) \quad \text{subject to the constraint} \quad k \geq 0.$$

Discretizing this system in time, using an implicit scheme, we can reformulate the

problem for each  $n$  as follows:

$$(15) \quad \text{minimize} \quad \|u^{n+1} - u^n\|,$$

$$(16) \quad \text{given} \quad k^{n+1} = k^n + \Delta t u_x^{n+1} \quad \forall n \geq 0,$$

$$(17) \quad \text{subject to the constraint} \quad k^n \geq 0 \quad \forall n \geq 0.$$

To simplify the notation, let  $\tilde{u} = u^{n+1}$ ,  $u = u^n$ , and  $k = k^n$ . Choosing to define the norm used on  $u_t$  as the 2-norm, our task is then to

$$(18) \quad \text{minimize} \quad \int (\tilde{u} - u)^2 dx,$$

$$(19) \quad \text{subject to} \quad k + \Delta t \tilde{u}_x \geq 0.$$

The corresponding variational principle states that there exist Lagrange multipliers  $\lambda(x) \leq 0$  such that

$$(20) \quad \delta \int \{(\tilde{u} - u)^2 + \lambda(x)(k + \Delta t \tilde{u}_x)\} dx = 0,$$

from which it follows (as shown in the appendix) that

$$2(\tilde{u} - u) = \Delta t \lambda_x \implies \frac{\tilde{u} - u}{\Delta t} = \frac{1}{2} \lambda_x.$$

The equivalent continuous statement is

$$(21) \quad u_t = \frac{1}{2} \lambda_x.$$

We will adopt the convention of writing the pressure as  $p = -\lambda/2$ . Our final system for the Lagrangian formulation of one-dimensional sea ice dynamics with constant thickness and without external forces is thus

$$(22) \quad k_t = u_x,$$

$$(23) \quad u_t = -p_x,$$

$$(24) \quad k \geq 0,$$

$$(25) \quad p \geq 0.$$

**5. The conundrum is unresolved: Introducing the concept of minimal pressure.** We have just derived a form for the pressure term as the  $x$ -derivative of a Lagrange multiplier. While this gives us the nice result that the pressure looks very much like the pressure for incompressible fluids, we still have little information about what the pressure actually is.

If we were able to resolve single floes, a constitutive law for frozen water would provide us with a way to calculate the pressure within each ice floe (provided that we know the external forces, including the pressure applied by other ice floes). Since we do not have resolution at this scale, however, we have to find a different method.

The pressure, constructed as a Lagrange multiplier, serves the purpose of enforcing the restriction that ice concentration cannot exceed 1 (or, equivalently,  $k$  cannot dip below 0). As long as  $k$  is far from 0, one would consequently expect  $p$  to equal 0. On the other hand, when  $k$  reaches 0,  $p$  needs to take on values to prevent it from decreasing further. (Note that this means that always one of  $k$  and  $p$  is zero.) There

is no reason, however, why it should push the ice apart, i.e., why the arising pressure should exceed the minimum necessary to satisfy the constraint. It is then a reasonable suggestion that the pressure should be calculated as the minimum necessary to enforce the constraint.

One should note at this point that in the more complex cases where  $h$  is allowed to vary, and in particular where crushing of the ice is permitted, this  $p$  needs to be limited by a maximal  $p$ . This is standard in other ice models (for two different formulations, see [3] and [8]). This extension for the minimization formulation for the pressure as we propose here will be discussed in Part 2.

Beyond the heuristic argument presented above, the formulation for the pressure as minimal suggested here is also mathematically appealing based on optimization theory. The first observation above (that  $\mathbf{k} \cdot \mathbf{p} = 0$ , where  $\mathbf{k}$  and  $\mathbf{p}$  denote the vectors of the respective discretized quantities) is nothing but the complementary slackness requirement of the Karush–Kuhn–Tucker conditions for constrained optimization problems.<sup>3</sup> Note also that because of (23), minimizing  $\|u_t\|_2$  is equivalent to minimizing  $\|p_x\|_2$ . Since  $p \geq 0$  and  $p = 0$  whenever  $k > 0$ , minimizing  $\|p_x\|_2$  is in turn equivalent to minimizing  $\|p\|_2$  or  $\|p\|_1$ , as will be shown below in section 7. It is thus natural to choose a formulation that aids in the calculations, and we will use the 1-norm of  $p$  to take advantage of available robust linear optimization techniques.

**6. An analytic solution to a well understood problem using jump conditions.** To build a better understanding of the form that the pressure takes, let us start by considering a problem whose solution we know from physical considerations. We take the half-infinite (one-dimensional) domain  $x \leq 0$ , with a wall at  $x = 0$ . Ice is initially distributed according to the given function  $k(0, x) = k_o(x)$  and moves according to  $u(0, x) = u_o(x)$ . We will assume that initially there are no patches of consolidated ice; i.e.,  $k_o(x) \neq 0 \forall x$ . If we assume that pressure arises inside the ice only when necessary, it follows that  $p(0, x) = 0 \forall x$ .

If anywhere in the domain  $u_x < 0$ , then the ice will accumulate somewhere until  $k = 0$  (or, equivalently,  $c = 1$ ). The wall at  $x = 0$  requires that  $u(t, 0) = 0 \forall t$ . Thus, a positive initial velocity anywhere will ensure ice accumulation.

The first problem we will consider has the first ice build-up occurring at the wall. (This can, for example, be achieved by setting  $u_o(x) \equiv u_o = \text{constant} > 0$ .) At the edge of the consolidated ice, a discontinuity in both concentration and velocity arises. We denote the location of this shock, marking the interface between the region with  $k = 0$  ( $c = 1$ ) and that with  $k > 0$  ( $c < 1$ ), by  $x = x_c$  and the time when this shock first forms by  $t = t_c$ ; i.e.,

$$(26) \quad t_c = \min \{t : k(t, x) = 0 \text{ for some } x < 0\},$$

$$(27) \quad x_c(t) = \min \{\tilde{x} : k(t, \tilde{x}) = 0 \forall x \geq \tilde{x}\}.$$

For  $t < t_c$ ,  $p(t, x) = 0 \forall x$ . The equations we solve for this portion are the very

---

<sup>3</sup>Physically, pressure is generally defined only up to a constant, since only its gradient enters into the dynamics. Similarly, here it is easy to see that adding an arbitrary (positive) constant to a  $p$  which solves the system (22)–(25) yields another solution. Strictly speaking, the KKT conditions do not necessitate  $p \geq 0$  and  $\mathbf{k} \cdot \mathbf{p} = 0$ ; they do provide for the *existence* of a  $p$  satisfying these conditions and solving the system (22)–(25). Hence we will choose the arbitrary constant such that they hold and  $\min p = 0$ .

simple set

$$(28) \quad k_t = u_x,$$

$$(29) \quad u_t = 0,$$

whose solution is

$$(30) \quad k(t, x) = k_o(x) + t u_{ox}(x),$$

$$(31) \quad u(t, x) = u_o(x),$$

$$(32) \quad p(t, x) = 0.$$

Assuming no consolidation except at the wall, this solution holds on  $\{(t, x) : t < t_c \text{ or } x < x_c\}$ . Once a region of consolidated ice starts to form along the wall, we know that for  $x > x_c$ ,

$$(33) \quad k(t, x) = 0,$$

$$(34) \quad u(t, x) = 0.$$

Thus, for  $t > t_c$  and  $x > x_c$ ,

$$(35) \quad u = 0 \implies u_t = 0 \implies p_x = 0 \implies p(t, x) = p(t).$$

In other words,  $p$  is constant throughout the region of consolidation at a given point in time.

The only unknowns are  $p$  and  $x_c$ . While the solutions to the left and to the right of  $x_c$  are smooth, there is a discontinuity, both in  $k$  and in  $u$ , at  $x_c$  itself. Using the corresponding jump conditions, we can calculate  $p$  and  $x_c$ .

Equations (22) and (23), respectively, imply that

$$(36) \quad \llbracket k \rrbracket \dot{x}_c = -\llbracket u \rrbracket,$$

$$(37) \quad \llbracket u \rrbracket \dot{x}_c = \llbracket p \rrbracket,$$

where  $\llbracket \cdot \rrbracket$  denotes the jump across the shock and  $\dot{x}_c$  is the shock speed. It follows from (36) that

$$(38) \quad \dot{x}_c = -\frac{\llbracket u \rrbracket}{\llbracket k \rrbracket} = -\frac{u_o(x_c)}{k_o(x_c) + t u_{ox}(x_c)}.$$

Together with the initial condition provided by evaluating (27) at  $t_c$ , this completely determines  $x_c$ . Combining (36) and (37), we find

$$(39) \quad \llbracket p \rrbracket = -\frac{\llbracket u \rrbracket^2}{\llbracket k \rrbracket} \implies p(t, x) = \frac{[u_o(x_c)]^2}{k_o(x_c) + t u_{ox}(x_c)} \quad \text{for } x > x_c.$$

One should note that this procedure of analyzing jump conditions to determine the pressure can easily be extended to examples with the consolidated ice not against a wall or with multiple consolidated regions. However, such an approach quickly becomes unmanageable, as the number of coupled nonlinear equations increases with the number of consolidated regions (two for each discontinuity, i.e., four for any region not against a wall). Besides, the locations of the interfaces between consolidated and nonconsolidated areas would need to be tracked, a laborious enterprise. Instead we want to use the minimal pressure hypothesis, which simplifies the calculations by making them global and, in the language of numerical conservation laws, is *capturing* rather than *tracking* the boundaries of the consolidated regions.

**7. Pressure minimization and norm comparison.** The toy problem we consider for a first validation of the minimal pressure hypothesis follows the example described in the previous section: Ice is moving towards a coast, where it consolidates and pressure builds up. We discretize (22) and (23) using a staggered grid and a backward Euler scheme as follows:

$$(40) \quad k_j^{n+1} = k_j^n + \frac{\Delta t}{\Delta x} \left( u_{j+\frac{1}{2}}^{n+1} - u_{j-\frac{1}{2}}^{n+1} \right),$$

$$(41) \quad u_{j+\frac{1}{2}}^{n+1} = u_{j+\frac{1}{2}}^n - \frac{\Delta t}{\Delta x} (p_{j+1}^{n+1} - p_j^{n+1}).$$

The constraints are

$$(42) \quad k_j^{n+1} \geq 0 \quad \forall j, n,$$

$$(43) \quad p_j^{n+1} \geq 0 \quad \forall j, n.$$

Note that it is necessary to use an implicit scheme for the evolution equation of  $k$ , in order to be able to satisfy the constraint. As  $p$  does not have an evolution equation, it is immaterial whether we use an explicit scheme or an implicit scheme for the  $u$ -equation. We have chosen to write it implicitly for consistency.

We place the wall at  $j = 5$ . As boundary conditions, we take that  $p_{-1}^{n+1} = p_0^{n+1} = 0$  (until the shock reaches this boundary) and  $p_5^{n+1} = p_4^{n+1} \forall n$ . As initial conditions, we assume that the shock is located at  $j = 2.75$ . To the left of the shock,  $p = 0$ ,  $k = 1/2$ , and  $u = 1$ . To the right of the shock,  $k = 0$  and  $u = 0$ .  $\Delta t$  is set to 0.5, and  $\Delta x$  is set to 1. (This allows us to capture the shock, which travels with speed 2. Of course, this resolution is very coarse. However, it serves to illustrate the point in this toy example.)

After the first time step,

$$(44) \quad u_{j+\frac{1}{2}}^1 = \begin{cases} 1 - \frac{1}{2} (p_{j+1}^{n+1} - p_j^{n+1}) & \text{if } j < 3, \\ -\frac{1}{2} (p_{j+1}^{n+1} - p_j^{n+1}) & \text{if } j \geq 3. \end{cases}$$

So the constraints (42) take the following form:

$$(45) \quad k_0^1 = \frac{1}{2} - \frac{1}{4} [p_1^1 - 2p_0^1 + p_{-1}^1] \geq 0,$$

$$(46) \quad k_1^1 = \frac{1}{2} - \frac{1}{4} [p_2^1 - 2p_1^1 + p_0^1] \geq 0,$$

$$(47) \quad k_2^1 = \frac{1}{2} - \frac{1}{4} [p_3^1 - 2p_2^1 + p_1^1] \geq 0,$$

$$(48) \quad k_3^1 = 0 - \frac{1}{2} - \frac{1}{4} [p_4^1 - 2p_3^1 + p_2^1] \geq 0,$$

$$(49) \quad k_4^1 = -\frac{1}{4} [p_5^1 - 2p_4^1 + p_3^1] \geq 0.$$

Now we have a system of five inequalities constraining  $p_1$ ,  $p_2$ ,  $p_3$ , and  $p_4$ . (Recall that  $p_{-1} = p_0 = 0$  and  $p_5 = p_4$ .) Minimizing the 2-norm of  $p_x$  while satisfying these

constraints gives for  $T = \Delta t$  that

$$\begin{aligned} p_0^1 &= 0, & k_0^1 &= \frac{1}{2}, & u_{.5}^1 &= 1, \\ p_1^1 &= 0, & k_1^1 &= \frac{1}{2}, & u_{1.5}^1 &= 1, \\ p_2^1 &= 0, & k_2^1 &= 0, & u_{2.5}^1 &= 0, \\ p_3^1 &= 2, & k_3^1 &= 0, & u_{3.5}^1 &= 0, \\ p_4^1 &= 2, & k_4^1 &= 0, & u_{4.5}^1 &= 0. \end{aligned}$$

From the jump conditions (cf. (39)) it follows that to the right of the shock

$$(50) \quad p = 2.$$

The shock speed can be calculated from (36) or (37) to be

$$(51) \quad \dot{x}_c = -2.$$

Thus the solution obtained by minimizing  $\|p_x\|_2$  is exactly what the analytic solution predicts: After time  $\Delta t = 0.5$ , the shock traveled one step to the left, with  $u$  and  $k$  retaining the same values on either side of the shock, while  $p = 2$  to the right of the shock. Similarly satisfying results were obtained for longer runs and for different initial conditions. In cases where the discretization does not allow for capturing the location of the shock exactly, a certain amount of numerical smoothing around the shock occurs, with  $p$ ,  $k$ , and  $u$  taking on intermediate values.

The three norms we want to compare are

1. the 2-norm of  $p_x$ , i.e.,  $\sum(p_i - p_{i-1})^2$ ,
2. the 2-norm of  $p$ , i.e.,  $\sum p_i^2$ ,
3. the 1-norm of  $p$ , i.e.,  $\sum |p_i|$ .

There are, of course, many other possible norms. These are some of the most natural choices and can be optimized with existing tools.

Solving the same problem above, but minimizing the 1- or 2-norm of  $p$ , gives exactly the same answer. This suggests that the norm chosen (at least from among these three) does not impact the result. In fact, this can be shown as follows.

First, consider  $\|p_x\|_2$ , with the additional condition that  $\min p = 0$  (see footnote 3). Recall that the KKT conditions then require  $p = 0$  when  $k > 0$ . Minimizing one of the norms of  $p$  itself also calls for  $p$  to be 0 whenever possible, in particular whenever  $k > 0$ .

Within regions of consolidated ice, where  $k = 0$ , we know that  $k_t \geq 0$ , and hence, by (22),  $u_x \geq 0$ .

(i) If  $u_x > 0$ , then  $k_t > 0$  and  $p_x = 0$  is a solution. (Physically, this is the situation where the consolidated ice is being pulled apart without the pressure acting.)

(ii) If  $u_x = 0$ , then  $u_{xt} \geq 0 \implies p_{xx} \leq 0$  (by (23)).

The values of  $p$  at the endpoints of the consolidated region are determined by the jump conditions, which have to be satisfied because of the constraining equations. Minimizing  $\|p\|$ , either as a 2-norm or as a 1-norm, with  $p_{xx} \leq 0$  requires  $p$  to be linear within the consolidated region. The same is true for  $\|p_x\|_2$ . (Note, however, that minimizing the 1-norm of  $p_x$  leads to nonunique solutions, where the one found using the other norms is but one possibility.)

Thus, for any of the three norms:

- (i)  $p = 0$  outside consolidated regions.
- (ii)  $p$  at the boundaries of consolidated regions is prescribed by the jump conditions imposed by the constraining equations.
- (iii)  $p$  is linear within consolidated regions.

It follows that the solutions are exactly the same.

As mentioned before, we have decided for our numerical work to rely on the 1-norm of  $p$  in order to facilitate the numerical optimization.

**8. The numerical model and another test case.** Our one-dimensional Lagrangian ice dynamics model for ice with uniform and constant thickness and without forcing is based on the discretization (40)–(43). For the optimization step, we use either Matlab’s built-in function `linprog` or a self-coded simplex method.

The problem described above (ice flowing towards a wall) can be successfully modeled this way (also with much better resolution and different initial conditions). We have also modeled, as another example, the case of a periodic domain, with initially uniformly distributed ice. The initial velocity function is sinusoidal with average velocity 0. Again, our physical intuition tells us what the solution should be: We expect the ice to consolidate in the middle of the domain. This is indeed what happens; see Figure 1. Given the initial conditions, we can also analytically calculate the first consolidation time, which in this case is  $1/4\pi \approx 0.0796$ . Again, the numerical results agree, predicting the first time for  $c = 1$  to lie in the interval  $[0.07875, 0.08]$  when a temporal step size of 0.00125 was chosen. The comparison of norms was again carried out in this model, which confirmed the previous conclusion that they yield the same answer, whereby minimizing the 1-norm of  $p$  is calculationally the least expensive. Various other initial conditions for  $u$ , including nonsymmetric cases, were studied, with the numerical results agreeing with the analytic solution (as far as this was easily obtained) and/or physical intuition.

**9. Another validation: Comparison with a particle-based method.** Further evidence in favor of the minimal pressure hypothesis comes from a comparison with a particle-based model. Here the one-dimensional sea ice motion is simulated as the interaction of individual “particles” (i.e., floes). Each of these is traced through space and time. Collisions are required to be mass- and momentum-conserving and inelastic (again following the observation that the pressure arising from collisions and consolidation does not lead to divergence). This is a rather costly method of modeling sea ice dynamics. However, for the purposes of validation, it is useful. After making the appropriate transformations from the respective coordinate system of each model to Eulerian coordinates, the concentration distributions resulting from the particle-based model and the continuum model with the minimal pressure hypothesis were compared, exhibiting remarkable agreement.

For the comparison, all external forces as well as crushing were again ignored. The initial concentration was taken to be constant  $c_o$  throughout the (periodic) domain. This is implemented in the collision model by an even spacing of identical particles. The number of particles corresponds to the resolution; the initial concentration determines the width of each particle. Later, the concentration is calculated at a particle point as the average area coverage between neighboring particles, i.e., at the point  $k$

$$(52) \quad c(k) = \frac{2w}{x(k+1) - x(k-1)},$$

where  $w$  is the width of a parcel,  $c(k)$  is the concentration, and  $x(k)$  is the location of the  $k$ th parcel. The velocities are tracked for each particle. They remain constant

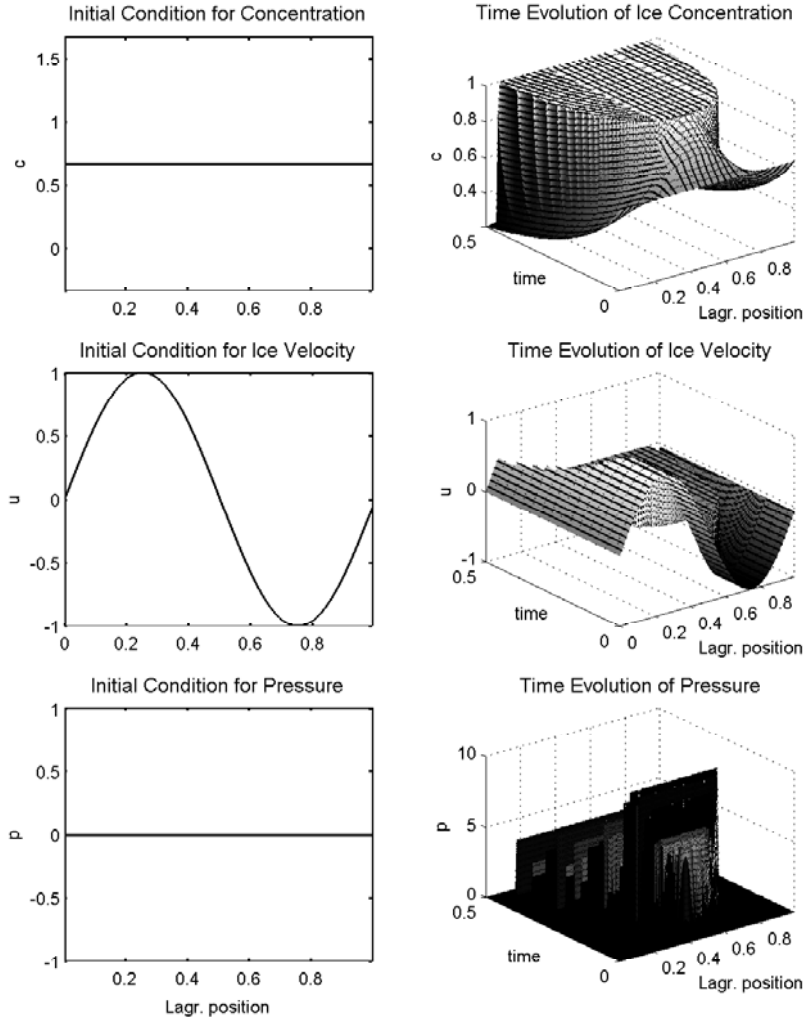


FIG. 1. The numerical results for ice consolidating in the center of the domain. Initial conditions are given in the plots on the left. The evolution is exhibited in the plots on the right. Note that the  $x$ -coordinate here is the Lagrangian position.

unless a collision occurs, in which case momentum conservation dictates the new velocity of the consolidated region: For particles  $j_1$  through  $j_2$  involved in the collision, each will have new velocity

$$(53) \quad u_{new} = \frac{\sum_{i=j_1}^{j_2} m_i u_i}{\sum_{i=j_1}^{j_2} m_i},$$

where  $u_i$  denotes the velocity of the  $i$ th particle and  $m_i$  its mass. Here, as in the continuum model, constant thickness is assumed. Hence the concentration  $c(i)$  is proportional to the mass  $m_i$  and can be substituted for it in the formula (53).

The initial velocity for both model runs was taken to be sinusoidal again, given

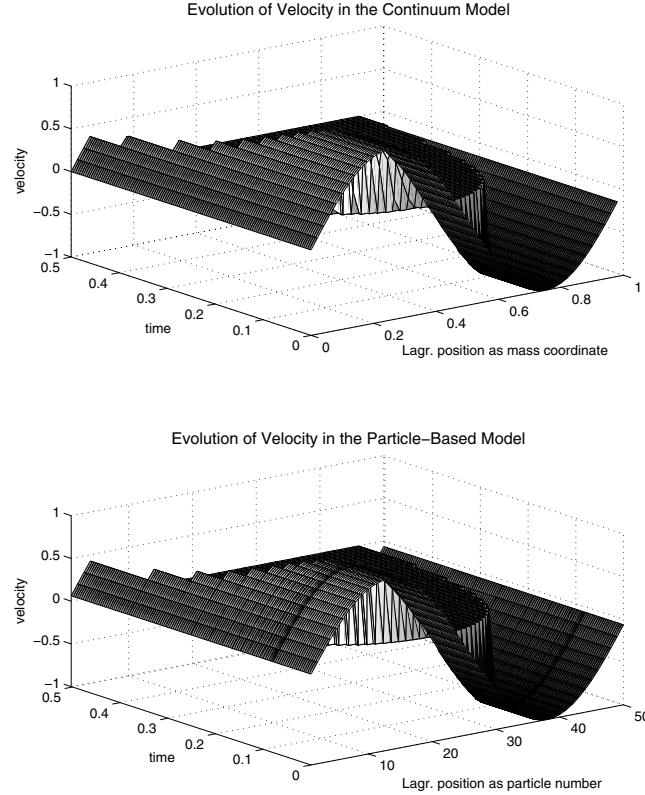


FIG. 2. The velocity evolutions derived by the continuum model using the minimal pressure hypothesis (top frame) and the particle-based model (bottom frame). Note that the x-coordinates here are the Lagrangian x-coordinates of each model.

in Eulerian coordinates as  $u_i^E(x) = \sin(2\pi c_o x)$ . (Note that this is equivalent to the case presented in the previous section. In the Lagrangian mass coordinates used there, the same velocity is written as  $u_i^L(\xi) = \sin(2\pi \xi)$ , where we are reverting to the Greek notation for clarification.) Two comparisons were carried out, one of the resulting velocity fields, the other of the resulting concentration fields. The Lagrangian coordinates of the continuum model with the minimal pressure hypothesis can be converted to Eulerian coordinates by numerically integrating the velocity  $u$  in time; the Eulerian positions of the particles in the collision model are recorded at each step.

Figure 2 shows the evolution of the velocities from the two models over 125 time steps. They are clearly very similar. A more detailed comparison is given in Figure 3. Here the Lagrangian coordinates are converted to Eulerian ones, and two different times are chosen. Note that in both plots, the velocities agree almost exactly. The one point of the particle model overshooting the continuum model (both in the positive and negative directions) in each plot is simply not resolved by the continuum model.

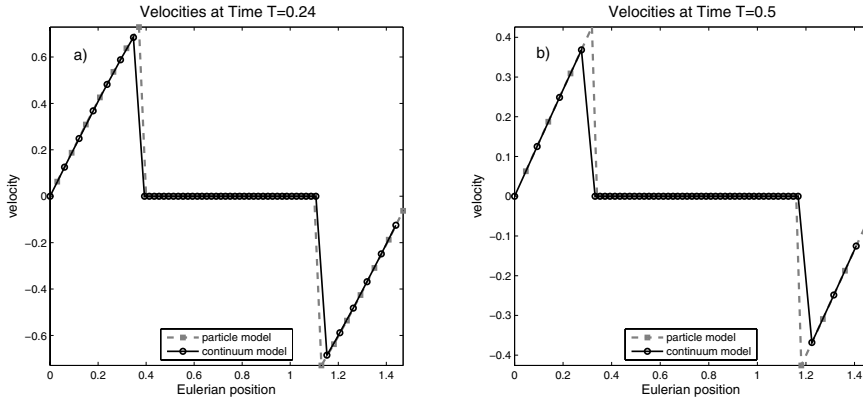


FIG. 3. The velocities derived with the continuum (solid line, circles) and the particle (dashed line, squares) models are compared at (a) an intermediate time and (b) the end of the run. The x-coordinates here are Eulerian x-coordinates.

Figure 4 shows the evolution of the concentrations from the two models over the 125 time steps. Again, a close similarity is apparent. To compare the concentration fields more exactly, we have chosen two points in time, one at the first collision (marked in the continuum model as the first time with nonzero pressure), the other at the end of the run. The results are shown in Figure 5. Up to the first collision, the concentration fields are identical between the two models. Recall that this time can be found analytically to be  $\frac{1}{4\pi} \approx 0.0796$ . With the resolution used here ( $\Delta t = 0.004$ ,  $\Delta\xi = 0.02$ ), the continuum model places it in the interval [0.076, 0.080], while the particle model predicts that the first collision will occur at time 0.0796. In other words, both models are in good agreement with the exact value. At time  $T = 0.5$ , small differences in the concentration fields are discernible. However, once again much of this difference can be ascribed to the fact that the two models do not resolve the same points.

One can conclude then that the model suggested here, using a minimization technique to calculate internal pressure, which is used in turn to update the velocity field, produces results entirely consistent with the physical description of sea ice motion as the interaction of ice floes through inelastic collisions.

**10. Conclusions.** We propose here a new closure for the equations of motion for sea ice modeled as a fluid. In addition to the momentum and the mass conservation equations, an expression for the internal forcing due to pressure has to be found. Based on the observation that collisions of ice floes at natural speeds tend to be inelastic, it was hypothesized that the internal pressure should stay at the minimum required to enforce a concentration of at most 1. This formulation is also consistent with treating the pressure as a Lagrange multiplier in the optimization problem minimizing the deviation from the unforced path under the constraints of the mass conservation equation and the limits on the concentration ( $0 \leq c \leq 1$ ).

To investigate the validity of this closure, a one-dimensional Lagrangian model was set up. Two classes of test cases were studied, ice moving towards a wall with initially constant velocity and ice moving in a periodic domain with initially sinusoidal velocity. Thickness was held constant for easier identification of the effects of the minimal pressure hypothesis, an assumption that will be relaxed in Part 2. For the

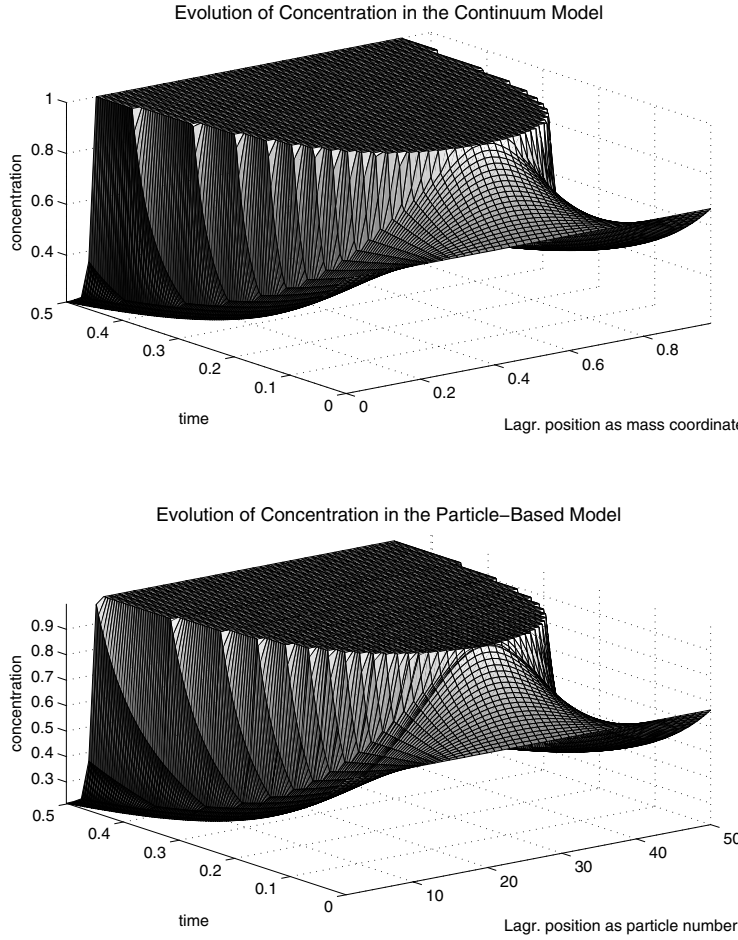


FIG. 4. The concentration evolutions derived by the continuum model using the minimal pressure hypothesis (top frame) and the particle-based model (bottom frame). Note that the x-coordinates here are the Lagrangian x-coordinates of each model.

first case, an exact analytic solution was derived—which was reproduced to high accuracy by the model (except for smoothing of the shock when the resolution was too coarse). The second case produced results consistent with physical intuition. A further validation was given by comparison with a particle-resolving model using inelastic collisions. Within the limits of their respective resolutions, the output of these two models was in exact agreement.

It is thus possible to conclude that the minimal pressure hypothesis leads to correct solutions, at least in the cases studied here. This is promising, because the work presented here forms the basis for more complex versions of the dynamics model using the minimal pressure hypothesis. The next step—a translation to Eulerian coordinates, allowing variable ice thickness, and implementing a finite ice strength—is presented in Part 2. Clearly, further study is required to determine the usefulness of this approach in large-scale simulations. Thus, for modeling real situations, an

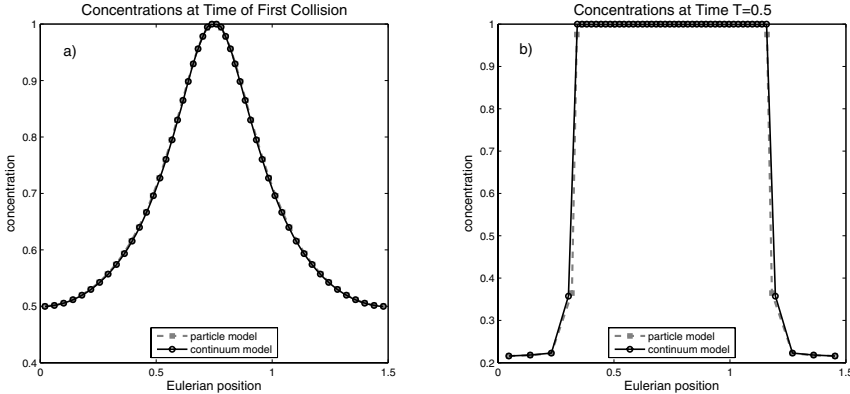


FIG. 5. The concentrations derived with the continuum (solid line, circles) and the particle (dashed line, squares) models are compared at (a) the time of first collision and (b) the end of the run. The  $x$ -coordinates here are Eulerian  $x$ -coordinates.

extension to two dimensions is necessary. Restoring the other forcing terms will be a minor task. The good agreement of the model results so far with analytic and particle-resolving model solutions justifies such further investigations, currently underway.

### Appendix. Derivations.

**A.1. Lagrangian equations.** Recall that (7) defined the Lagrangian coordinates as

$$\begin{cases} \xi = \int_0^x ch d\hat{x}, \\ \tau = t. \end{cases}$$

The partial derivatives relating them to the Eulerian coordinates  $(t, x)$  are as follows:

$$(54) \quad \frac{\partial \xi}{\partial x} = ch,$$

$$(55) \quad \frac{\partial \xi}{\partial t} = -chu,$$

$$(56) \quad \frac{\partial \tau}{\partial x} = 0,$$

$$(57) \quad \frac{\partial \tau}{\partial t} = 1,$$

where (4) was used for the partial derivative  $\partial \xi / \partial t$ . Similarly,

$$(58) \quad \frac{\partial x}{\partial \xi} = \frac{1}{ch},$$

$$(59) \quad \frac{\partial x}{\partial \tau} = u,$$

$$(60) \quad \frac{\partial t}{\partial \xi} = 0,$$

$$(61) \quad \frac{\partial t}{\partial \tau} = 1,$$

Now consider  $u = u(t(\tau, \xi), x(\tau, \xi))$ :

$$\begin{aligned}\frac{\partial u}{\partial \tau} &= u_t t_\tau + u_x x_\tau \\ &= u_t + u_x u \\ &= F \quad \text{from (5).}\end{aligned}$$

This is (9).

Following the same pattern, we find

$$\begin{aligned}\frac{\partial u}{\partial \xi} &= u_t t_\xi + u_x x_\xi \\ &= \frac{u_x}{ch} \\ &= -\frac{1}{(ch)^2} [-(ch)u_x] \\ &= -\frac{1}{(ch)^2} [(ch)_t + (ch)_x u] \quad \text{from (4)} \\ &= -\frac{1}{(ch)^2} [(ch)_t t_\tau + (ch)_x x_\tau] \\ &= \left( \frac{1}{ch} \right)_\tau.\end{aligned}$$

This yields (8).

**A.2. Solution to the variational problem.** The variational problem posed in section 4 is

$$\delta \int \{ (\tilde{u} - u)^2 + \lambda(x)(k + \Delta t \tilde{u}_x) \} dx = 0.$$

Equivalently,

$$\begin{aligned}\forall f \in C_o^\infty, \quad 0 &= \frac{d}{d\epsilon} \Big|_{\epsilon=0} \int \left[ (\tilde{u} + \epsilon f - u)^2 + \lambda \left( k + \Delta t \frac{\partial}{\partial x} (\tilde{u} + \epsilon f) \right) \right] dx \\ &= \int [2\tilde{u}f - 2uf + \Delta t \lambda f_x] dx \\ &= \int f [2(\tilde{u} - u) - \Delta t \lambda_x] dx,\end{aligned}$$

which implies that

$$2(\tilde{u} - u) = \Delta t \lambda_x.$$

**Acknowledgments.** We would like to thank David Holland for many fruitful conversations on the subject of sea ice dynamics, and Oliver Bühler for stimulating suggestions. We are also grateful to the anonymous reviewer for the valuable comments.

## REFERENCES

- [1] T. E. ARBETTER, J. A. CURRY, AND J. A. MASLANIK, *Effects of rheology and ice thickness distribution in a dynamic-thermodynamic sea ice model*, J. Phys. Oceanogr., 29 (1999), pp. 2656–2670.
- [2] G. M. FLATO AND W. D. HIBLER, III, *Modeling pack ice as a cavitating fluid*, J. Phys. Oceanogr., 22 (1992), pp. 626–651.
- [3] W. D. HIBLER, III, *A dynamic thermodynamic sea ice model*, J. Phys. Oceanogr., 9 (1979), pp. 817–846.
- [4] M. A. HOPKINS, *On the mesoscale interaction of lead ice and floes*, J. Geophys. Res., 101 (1996), pp. 18315–18326.
- [5] E. C. HUNKE AND J. K. DUKOWICZ, *An elastic-viscous-plastic model for sea ice dynamics*, J. Phys. Oceanogr., 27 (1997), pp. 1849–1867.
- [6] C. F. IP, W. D. HIBLER, III, AND G. M. FLATO, *On the effect of rheology on seasonal sea-ice simulations*, Ann. Glaciol., 15 (1991), pp. 17–25.
- [7] M. KREYSCHER, M. HARDER, P. LEMKE, AND G. M. FLATO, *Results of the sea ice model inter-comparison project: Evaluation of sea ice rheology schemes for use in climate simulations*, J. Geophys. Res., 105 (2000), pp. 11299–11320.
- [8] J. E. OVERLAND AND C. H. PEASE, *Modeling ice dynamics of coastal seas*, J. Geophys. Res., 93 (1988), pp. 15619–15637.
- [9] H. SCHAFFRIN, *An Optimization Approach to Sea Ice Dynamics*, Ph.D. thesis, Department of Mathematics, Courant Institute of Mathematical Sciences, New York University, New York, NY, 2005.
- [10] A. S. THORNDIKE, D. A. ROTHROCK, G. A. MAYKUT, AND R. COLONY, *The thickness distribution of sea ice*, J. Geophys. Res., 80 (1975), pp. 4501–4513.
- [11] L.-B. TREMBLAY AND L. A. MYSAK, *Modeling sea ice as a granular material, including the dilatancy effect*, J. Phys. Oceanogr., 27 (1997), pp. 2342–2360.
- [12] B. ZHANG, *On a local existence theorem for a simplified one-dimensional hydrodynamic model for semiconductor devices*, SIAM J. Math. Anal., 25 (1994), pp. 941–947.